Spin-polarized photoemission of $Fe_{80}B_{20}$

Y B Xu†, C G H Walker†‖, D Greig†, E A Seddon‡, L W Kirkman‡,
F M Quinn‡ and J A D Matthew§

† Department of Physics, The University of Leeds, Leeds LS2 9JT, UK
‡ Daresbury Laboratory, Daresbury, Warrington, Cheshire WA4 4AD, UK
§ Department of Physics, The University of York, Heslington, York YO1 5DD, UK

Abstract. The first spin-resolved photoemission experiment on an iron–boron amorphous alloy using a synchrotron source is presented. The experimental spin polarization of the d band of $Fe_{80}B_{20}$ has been compared with three theoretical predictions and found to be in best agreement with self-consistent spin-polarized calculations based on a supercell LMTO approach. The observed average spin polarization of the valence band is approximately twice that of 10 eV secondary electrons. Hysteresis loops for $Fe_{80}B_{20}$ determined from the 1 eV and 20 eV secondary-electron asymmetry are similar to those determined using the magnetooptic Kerr effect, but show a lower coercivity. The differences are attributed to a combination of different sampling depths of the two techniques and to the surface inhomogeneity of the sample.

1. Introduction

Ferromagnetic transition metal amorphous glasses continue to be of interest both as model systems for understanding electronic structure in amorphous metals and as prototypes of technologically important magnetic alloys. Recent spin-polarized band calculations of amorphous Fe_xB_{100-x} by Hafner *et al* [1] have combined improved structural modelling using molecular dynamics with enhanced self-consistency based on a supercell linear-muffin-tin-orbital approach. This is to be compared with the 'average atom' self-consistency achieved by Nowak *et al* [2] and Bratkovsky and Smirnov [3] and previous non-self-consistent tight-binding approaches such as that of Krompiewski *et al* [4, 5]. Although all of these methods lead to the same general picture, namely a non-bonding non-spin-polarized B 2s band lying below a strongly hybridized spin-polarized Fe d/B p band as in crystalline iron, there are important differences in detail. Hafner *et al* [1] predict negative local iron moments at some sites for boron concentrations of less than 20% indicating competition between antiferromagnetic and ferromagnetic coupling. Although all models give split d-band behaviour reminiscent of e_g/t_{2g} splitting in cubic iron, the magnitude of the splitting and the relative shifts of up- and down-spin bands are model sensitive: for example the spin polarization at the Fermi edge may even differ in sign for different models.

Experimental tests of the theoretical predictions are largely confined to measurements of average magnetic moments per iron atom, electronic specific heat and spin-averaged ultraviolet and x-ray photoemission (UPS and XPS) from the conduction band. Spin-resolved photoemission experiments are rare on amorphous metals: Hopster *et al* [6] have

‖ Current address: Department of Applied Biological and Chemical Sciences, University of Ulster, Cromore Road, Coleraine BT52 1SA, UK.

studied the spin-resolved densities of states of $Fe_xB_yX_z$ (X = Ni or Si) ferromagnetic metallic glasses using UPS ($h\nu = 21.2$ eV) but Fe_xB_{100-x} itself has received only scant attention [7].

In this paper we present the first spin-resolved photoemission experiment on iron–boron using a synchrotron source—comparing the observed spin polarization throughout the d band with the various theoretical predictions. In addition, the average spin polarization of the d band is correlated with that observed using secondary-electron emission [8], and the ferromagnetic hysteresis of the 1 eV and 20 eV secondary electrons is in turn compared with the hysteresis observed using the magnetooptical Kerr effect (MOKE) [9]. The similarities and differences between the magnetization parameters that emerge are related to the diverse sampling depths of these magnetic sensing techniques.

2. Experimental details

The experimental work reported here was performed on station 6.1 of the Synchrotron Radiation Source (SRS) at Daresbury Laboratory. The station, which is designed for UHV photoemission work in the photon energy range 80–180 eV, was modified for this spin-resolved work by the incorporation of a small hemispherical energy analyser and 'micro-Mott' polarimeter; these have been described in detail elsewhere [10–12]. A Sherman function of 0.15 was assumed for the polarimeter. The experimental relationship of the photon beam, the FeB ribbon sample and the polarimeter are shown schematically in figure 1.
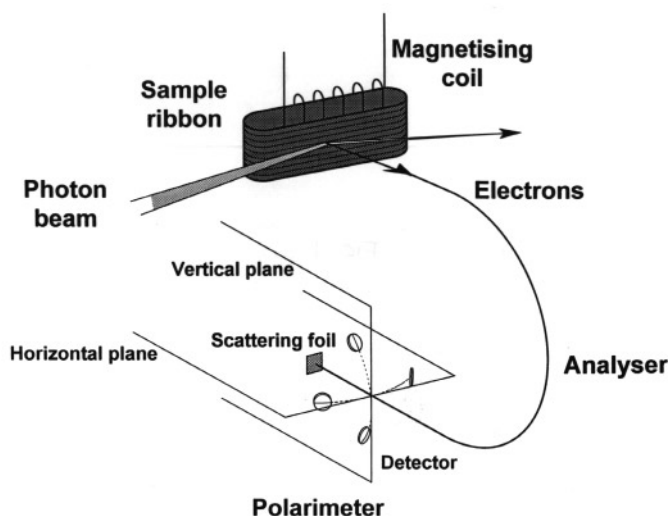

Figure 1. A schematic representation of the experimental arrangement.

The $Fe_{80}B_{20}$ which was prepared by melt spinning, was formed into a closed loop that could be magnetized by passing a small current through an insulated wire wrapped around the rear of the sample. It was cleaned *in situ* by argon ion bombardment until there was no evidence for oxygen contamination as judged by photoemission. Though oxygen free to the photoemission detection limit, the sample contained a significant quantity of carbon, the level of which was not reduced by further sputtering. *In situ* AES analysis was not very precise, but the sample was also studied by XPS in the RUSTI Scienta spectrometer at Daresbury

Laboratory. Following 20 min of Ar^+ ion bombardment very low signals were registered for both O and C, and the composition (assumed homogeneous) had stabilized to a level very close to the nominal 80:20 Fe:B values. The XPS measurements do, however, reflect composition at a depth of 10–20 Å, and so are less surface sensitive than the spin-polarized photoemission. The upper (shiny) surface of the ribbon was used for the measurements which were made at room temperature either in remanence or with a small dc current passing through the magnetizing coil. The sample was not annealed. Base pressures of 5×10^{-10} Torr were routinely obtained during this study.

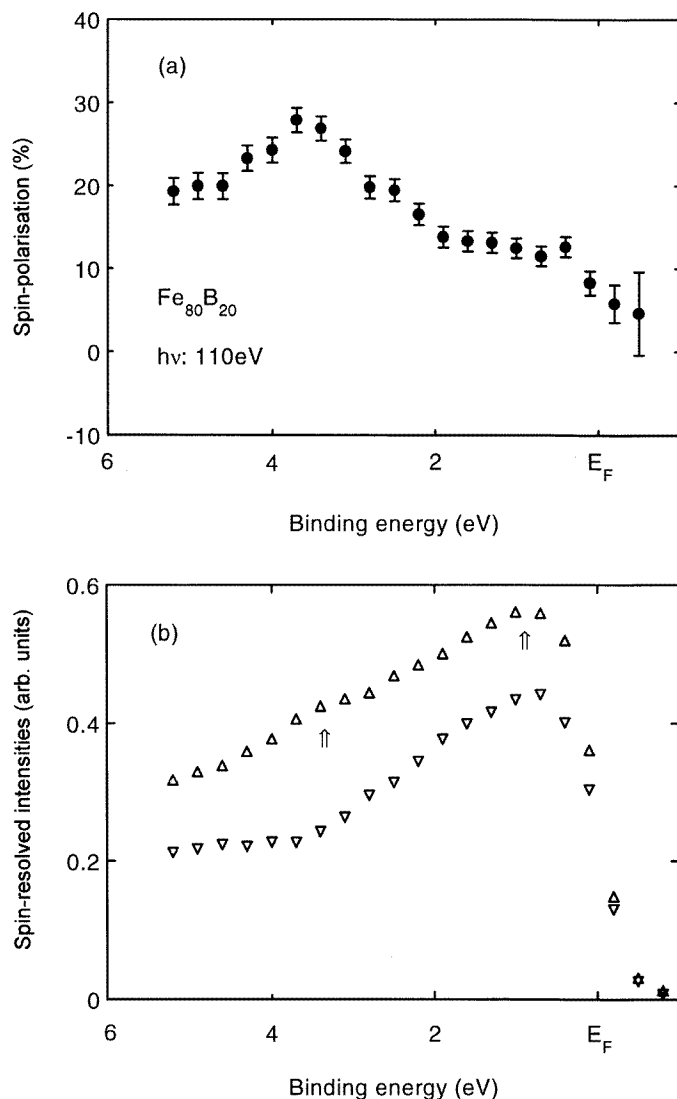**Figure 2.** (a) The observed spin polarization and (b) the SREDCs of the d band of amorphous $Fe_{80}B_{20}$ excited using 110 eV photons: $\triangle$, majority spin; $\triangledown$, minority spin.

3. Results

The experimental spin-integrated energy distribution curve (EDC) agrees well with previous studies at both lower and higher photon energies. In figure 2 we show (a) the observed spin polarization and (b) the spin-resolved EDC (SREDC) of the valence band of amorphous $Fe_{80}B_{20}$ obtained using a photon energy of 110 eV. This was chosen to give a reasonable cross-section and surface sensitivity, whilst at the same time producing photoelectrons of sufficient kinetic energy for the spin dependence of the mean free path to be insignificant. The spin dependence of the conduction band density of states then dominates the observed polarization. The SREDCs clearly show a spin imbalance throughout the 0–6 eV binding energy range, both majority and minority spin states being occupied at E_f. Results for other photon energies within the range of station 6.1 are very similar. The effect of subtracting linear-, Tougaard- or Shirley-type backgrounds [13] from the SREDCs has been investigated. In practice the spectral profiles that emerge were found to be relatively insensitive to the choice of background function with only slight differences in the magnitudes of the peaks.
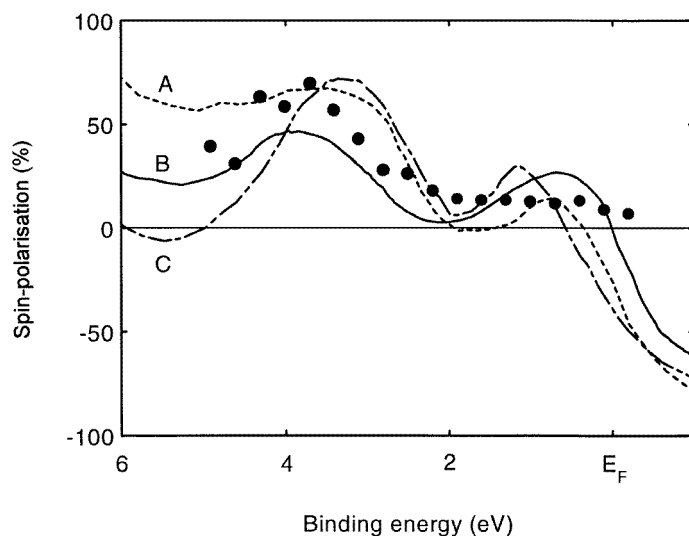

Figure 3. The theoretical and background-corrected experimental polarizations of $Fe_{80}B_{20}$: **A**, Nowak *et al* [2]; **B**, Hafner *et al* [1]; **C**, Bratkovsky and Smirnov [3], with circles representing the SREDCs from figure 2(b).

The predicted 0–6 eV electron polarizations, as shown by the curves in figure 3, were calculated from the theoretical spin-resolved DOS of $Fe_{80}B_{20}$ [1–3]. The circles in figure 3 are the background-corrected experimental values of polarization calculated from the SREDCs shown in figure 2(b). The theoretical polarizations are rather similar in their gross features, showing a two-peak profile but with maximum polarizations that span the range 40–70%. The two-peak structure was not clearly resolved experimentally although the polarization profile shows the same gross trends as predictions. However we note that some of the other details of the calculated polarizations are quite model dependent. For example the three predicted values of polarization close to E_f are quite different. With this in mind particular attention was paid to the experimental polarization close to E_f. Careful study revealed that the polarization stayed positive and this observation clearly supports the theoretical predictions of Hafner *et al* [1].

As spin is conserved during the direct photoemission process, and the escape depths for 50–100 eV electrons have weak spin dependence and are small (of the order of a few monolayers), the overall experimental polarization of the valence band is approximately proportional to the surface magnetization of the valence band [14]. In addition, it is now generally accepted that 10–20 eV secondary electron polarization is equal to the mean valence band polarization of the uppermost layers of the material. Rarely, however, are the polarizations of both the valence band photoemission *and* the secondary electrons reported for the same system. In a direct comparison between the two measurements we found that the polarization of the 10–20 eV secondary electrons is approximately *half* the magnitude of the average valence band polarization estimated from the background-corrected SREDCs in figure 2(b).

The contrasting forms of magnetic hysteresis loops obtained from $Fe_{80}B_{20}$, using (a) longitudinal MOKE [9], (b) the spin asymmetry of 1 eV secondary electrons and (c) the spin asymmetry of 20 eV secondary electrons, are shown in figure 4. In a point of similarity the hysteresis loops show 100% remanent magnetization for $Fe_{80}B_{20}$ regardless of the technique used to obtain them. On the other hand, the coercive fields determined for $Fe_{80}B_{20}$ are clearly technique dependent. The coercivities obtained from secondary-electron polarizations are approximately 20% smaller than those determined using MOKE. Furthermore, the hysteresis loops from the secondary electrons may be displaced with respect to the field axis, the 1 eV loop slightly so and the 20 eV loop prominently so as seen in figure 4. However, the extent of this effect does vary from sample to sample. The 20 eV loop is also more rounded.

The probing depth for MOKE is about 100 ML so the technique is essentially a bulk magnetism probe. The probing depth, λ, of the secondary electrons has been shown to be determined principally by electron–electron scattering, and, although the exact degree of the surface sensitivity of secondary electrons is debatable, their probing depth is clearly much shorter (for 20 eV electrons about 2–3 ML) than that of MOKE. The situation for the 1 eV cascade electrons is less clear. From the so-called universal curve [15] λ is about 10–20 ML for electrons with low kinetic energies (i.e. $E_k < 5$ eV) in non-magnetic systems. Recently, however, Siegmann [16] and Pappas *et al* [17] showed that in magnetic systems the *spin* memory is only a few monolayers, even for electrons with very low kinetic energy.

4. Discussion

The experiments presented here cast light on two aspects of the spin polarization of the densities of states in the conduction bands of amorphous iron boron alloys.

(i) Conduction band photoemission has been compared with the results of three recent theoretical predictions. We emphasize that the fine details of both the theoretical and experimental curves are sensitive to a number of assumptions. For example, although it is clear that photoemission is dominated by electrons originating in the Fe d-like states, the precise weighting of the cross-sections for components from the different partial densities of states is open to question. Similarly the value of the Sherman function used and ambiguities in background subtraction will affect the precise *magnitude* of spectral features although we emphasize that the *location* of these features is unaffected. In particular the presence of a distinct peak in the spin polarization in the binding energy range 3.0–3.7 eV is a robust feature with the experimental polarization in reasonable accord with theory for both spin-up and spin-down photoemission. From calculations it is clear that this feature arises from the presence of a modest peak in the spin-up density of states accompanied by a weak density of states for the spin-down electrons. Near the Fermi edge the experimental spin polarization
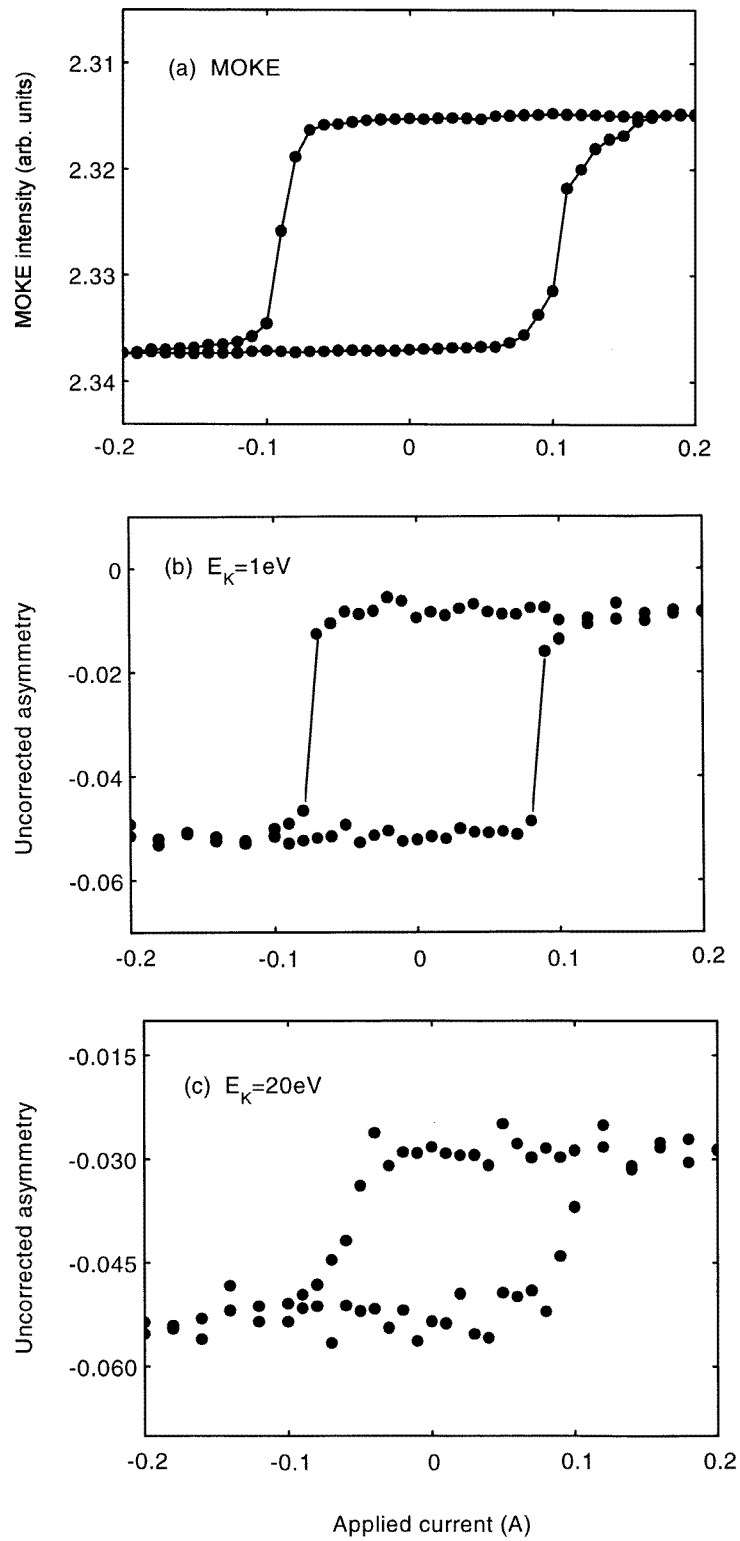
Figure 4. A comparison of magnetic hysteresis loops obtained using (a) the longitudinal MOKE, (b) the spin asymmetry of 1 eV secondary electrons and (c) the spin asymmetry of 20 eV secondary electrons.

is lower than predicted by theory. Nevertheless it remains positive at E_F, consistent with the recent theory of Hafner *et al* [1] and contrary to the earlier theories of Nowak *et al* [2] and Bratkovsky and Smirnov [3], both of which predict a negative polarization. The magnetic parameters of the material are all very sensitive to this property. Although there remains some uncertainty about the surface—as opposed to the bulk—composition of the sample, the results presented here provide some useful discrimination between different models of the spin-resolved structure of Fe$_{80}$B$_{20}$.

(ii) The spin polarization of the secondary electrons of Fe$_{80}$B$_{20}$ follows the pattern of previous experimental studies [18] as well as theoretical predictions [8]. At very low kinetic energy the polarization reflects both the spin polarization of the electrons excited from the conduction band and the spin dependence of the mean free path, but by 20 eV the former effect dominates. Both the experimental overall spin polarization of the conduction band ($\approx$ 17%) and the polarization of the secondary emission above 10 eV ($\approx$ 9%) are less than the conduction-band polarization of Fe$_{80}$B$_{20}$ predicted by theory, which, dependent upon the model, ranges from 21% to 27%. Whilst the absolute values of the experimental polarizations may be low owing to the assumed magnitude of the Sherman function, the fact that the conduction-band polarization is approximately twice that of the secondary electrons is significant. Naively it might be expected that both polarizations should follow that predicted for the conduction band; however the magnetic environment close to the surface is expected to be different from that of the bulk and, in addition, may have considerable inhomogeneity, owing to both topographical environments and possible compositional variations near the surface.

Although low saturation fields are observed in amorphous alloys due to the absence of crystalline anisotropy, the 100% remanence ratios of figure 4 show that *some* degree of anisotropy, possibly uniaxial stress anisotropy induced during ribbon formation, must be present. In negative fields the magnetization is reversed with the low coercivity in this 'soft' magnetic alloy largely determined by the pinning of the domain walls. The smaller coercivities obtained from the secondary electron measurements may indicate that structural or compositional changes at the surface lead to different forms of pinning or facilitate the growth of the reversal domains. The observed loop displacement may be due either to exchange anisotropy resulting from an iron-rich antiferromagnetically ordered layer at the surface (formed, for example, after sputter cleaning [19]) coupled to the ferromagnetically ordered bulk material [20, 21], or to differential stress anisotropy near the surface.

5. Conclusions

Synchrotron radiation at photon energies around 110 eV is an ideal probe of the spin dependence of both valence-band photoemission and secondary-electron emission. The observed spin polarization of the d band of Fe$_{80}$B$_{20}$ is in general accord with available theories, agreeing best with the theoretical predictions of Hafner *et al* [1]. The peak at about 3.7 eV binding energy arises from a peak/trough in the spin-up/spin-down densities of states. The average polarization of the valence band is about twice the polarization of secondary electrons in the energy range 10–20 eV. Hysteresis loops for Fe$_{80}$B$_{20}$ determined from 1 eV and 20 eV secondary-electron asymmetries are similar to those determined using the MOKE but may be asymmetrical and show lower values of coercivity. The differences are attributed to a combination of different sampling depths of the two techniques together with roughening and possible chemical inhomogeneity of the surface.

Acknowledgments

References

[1] Hafner J, Tegze M and Becker Ch 1994 *Phys. Rev.* B **49** 285
[2] Nowak H J, Anderson O K, Fujiwara T, Jepson O and Vargas P 1991 *Phys. Rev.* B **44** 3577
[3] Bratkovsky A M and Smirnov A V 1993 *J. Phys.: Condens. Matter* **5** 3203
[4] Krompiewski S, Krey U, Krauss U and Ostermeier H 1988 *J. Magn. Magn. Mater.* **73** 5
[5] Krompiewski S, Krey U, Krauss U and Ostermeier H 1987 *J. Magn. Magn. Mater.* **69** 117
[6] Hopster H, Kurzawa R, Raue R, Schmitt W Q, Guntherodt G, Walker K H and Guntherodt H J 1985 *J. Phys. F: Met. Phys.* **85** L11
[7] Colla E, Mauri D and Landolt M 1982 *Helv. Phys. Acta* **55** 177
[8] Penn D R, Apell S P and Girvin S M 1985 *Phys. Rev.* B **32** 7753
[9] Bader S D 1991 *J. Magn. Magn. Mater.* **100** 440
[10] Quinn F M, Seddon E A and Kirkman I W 1995 *Rev. Sci. Instrum.* **66** 1564
[11] Seddon E A, Kirkman I W and Quinn F M 1995 *Polarized Electron/Polarized Photon Physics* ed H Kleinpoppen and R Newell (New York: Plenum) p 95
[12] Kirkman I W, Seddon E A and Quinn F M *Daresbury Laboratory Report* DLTR 95/002
[13] Shirley D A 1972 *Phys. Rev.* B **5** 4709
[14] Siegmann H C 1992 *J. Phys.: Condens. Matter* **4** 8395
[15] Seah M P and Dench W A 1979 *Surf. Interface Anal.* **1** 2
[16] Siegmann H C 1994 *J. Electron. Spectrosc. Relat. Phenom.* **68** 505
[17] Pappas D P, Kamper K-P, Miller B P, Hopster H, Fowler D E, Brandle C R, Luntz A C and Shen Z X 1991 *Phys. Rev. Lett.* **66** 504
[18] Unguris J, Pierce D T, Galejs A and Celotta R J 1982 *Phys. Rev. Lett.* **49** 72
[19] See, for example, Hucknall P K, Walker C G H, Greig D, Matthew J A D, Norman D and Turton J 1992 *Surf. Interface Anal.* **19** 23
[20] Meiklejohn W H and Bean C P 1957 *Phys. Rev.* **105** 904
[21] Meiklejohn W H 1962 *J. Appl. Phys.* **33** 1328